Thickness-Dependent Reversible Hydrogenation of Graphene Layers

Zhiqiang Luo,[†,‡] Ting Yu,[†,*] Ki-jeong Kim,[§] Zhenhua Ni,[†] Yumeng You,[†] Sanhua Lim,[‡] Zexiang Shen,[†] Shanzhong Wang,[⊥] and Jianyi Lin[‡,*]

[†]Division of Physics and Applied Physics, School of Physical and Mathematical Sciences, Nanyang Technological University, Singapore 637371, [‡]Applied Catalysis, Institute of Chemical and Engineering Sciences, Singapore 62783, [§]Pohang Accelerator Laboratory, POSTECH, Pohang, Korea 790-784, and [⊥]STMicroelectronics Asia Pacific Pte Ltd, Singapore 554812

ABSTRACT In this work, graphene layers on SiO_2/Si substrate have been chemically decorated by radio frequency hydrogen plasma. Hydrogen coverage investigation by Raman spectroscopy and micro-X-ray photoelectron spectroscopy characterization demonstrates that the hydrogenation of single layer graphene on SiO_2/Si substrate is much less feasible than that of bilayer and multilayer graphene. Both the hydrogenation and dehydrogenation process of the graphene layers are controlled by the corresponding energy barriers, which show significant dependence on the number of layers. The extent of decorated carbon atoms in graphene layers can be manipulated reversibly up to the saturation coverage, which facilitates engineering of chemically decorated graphene with various functional groups *via* plasma techniques.

KEYWORDS: graphene · hydrogenation · plasma · Raman spectroscopy · X-ray photoelectron spectroscopy

Graphene, a two-dimensional crystal made of carbon atoms arranged in a honeycomb lattice, has attracted great attentions because of its exceptional properties since it was first discovered in late 2004.[1] In addition to its promising applications in future ultrahigh-speed nanoelectronics,[2] the purely two-dimensional atomic structure and high crystallinity make graphene an ideal candidate for use as chemical sensor and biosensor devices.[3,4] Similar to the modulation of chemical and physical properties of single-walled carbon nanotubes (SWNTs) using chemical modification in recent years,[5−8] the chemical modification of graphene, using a direct chemical grafting process, should be an effective way to functionalize its surface to further exploit the possibilities of graphene sensors.[4]

Gas-phase functionalization techniques would be extremely useful for the fabrication of sensor devices based on graphene.[6−8] Exposing SWNTs to atomic hydrogen generated C−H bonds on the surface of the SWNTs, results in an increase in the sp3 hybridization and an enhancement in the semiconducting characteristics of SWNTs.[7,8] Surface modification of graphene layers with various functional groups is also expected to alter transport properties that may lead to useful semiconducting devices.[9] In particular, the theoretical prediction of graphane, a fully hydrogenated single layer graphene, shows promising semiconductor properties.[10] Recently, Elias *et al*. demonstrated the control of the electrical transport properties of single layer graphene by a reversible hydrogenation process.[11] Their work shows the possibilities of conversion of graphene into new graphene derivatives with a regular structure by attaching exotic atoms on the carbon scaffold of graphene.[11]

In this paper, we present systematic experimental investigations of the surface modification of graphene sheets of one to five layers using hydrogen plasma treatment. The hydrogenation of bilayer and multilayer graphene is found to be much more feasible than that of single layer graphene on SiO_2/Si substrate by Raman spectra and micro-XPS spectra characterization. The hydrogenation barriers of the graphene layers show clear dependence on the number of layers. Moreover, it is revealed that there are two types of dehydrogenation mechanism with different dehydrogenation barriers, which exhibit different dependences on the number of graphene layers and the amount of the hydrogen coverage. With proper plasma power and exposure duration, hydrogen coverage on graphene layers could be manipulated up to the saturation state. Our intensive study of hydrogenation and dehydrogenation of graphene layers provides useful information for exploiting the decorated graphene by grafting exotic atoms and functional groups *via* plasma techniques, which will be an essential way to manipulate chemical and

*Address correspondence to yuting@ntu.edu.sg, lin_jianyi@ices.a-star.edu.sg.

Received for review April 14, 2009 and accepted May 25, 2009.

Published online June 3, 2009.
10.1021/nn900371t CCC: $40.75

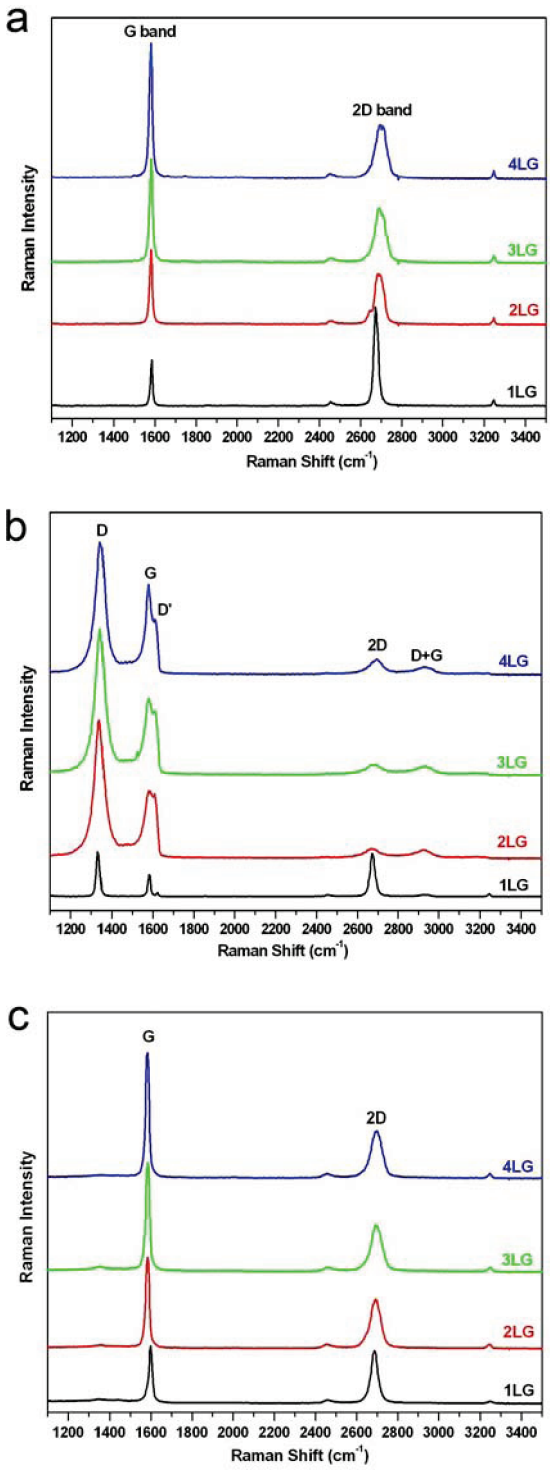

Figure 1. (a) Raman spectra of pristine 1LG, 2LG, 3LG, and 4LG; (b) Raman spectra of 1LG, 2LG, 3LG, and 4LG hydrogenated by 10 W, 1 Torr hydrogen plasma for 1 min; (c) Raman spectra of 1LG, 2LG, 3LG, and 4LG dehydrogenated by vacuum annealing.

physical properties of graphene for senor devices applications.

RESULTS AND DISCUSSION

The thickness of the graphene layers was identified using Raman and contrast spectrum technique.[12] Graphene layers with various layer numbers (1, 2, 3, 4, 5 and few layers) were simultaneously present in a single graphene flake. They were subjected to hydrogen plasma treatments and subsequent thermal heating under identical conditions so that hydrogenation and dehydrogenation as a function of the layer number can be compared directly. Figure 1a shows the Raman spectra of 1 to 4-layer graphene layers (*i.e.*, 1LG, 2LG, 3LG, 4LG) on the SiO_2/Si substrate prior to the hydrogenation treatments. The two intense peaks, G band at ~1580 cm^{-1} and 2D band at ~2700 cm^{-1} are characteristic of graphene samples,[13,14] due to the in-plane vibrational (E_{2g}) mode and the two phonon intervalley double resonance scattering, respectively. The 2D band of one-layer graphene is very sharp and strong. The increase in layer numbers leads to significant broadening of the width and blue-shift of the 2D band, which could function as the fingerprint in distinguishing the 1LG, 2LG, and multilayer graphene.[14,15] The intensity of G band increases almost linearly with the increasing number of graphene layers.[16]

After hydrogen plasma treatment (10 W, 1 Torr, 1 min), the Raman spectra of the graphene sample change significantly. As shown in Figure 1b, three new peaks at 1340, 1620, and 2920 cm^{-1} are observable in all the Raman spectra of the hydrogenated graphene layers. The peak at 1340 cm^{-1} is assigned to D band, which is not detected in disorder-free graphene and requires defects for its activation *via* an intervalley double-resonance Raman process.[17] Commonly the relative intensity of D band can serve as a convenient measure for the amount of defects in graphene. D band is very sharp with a full width at half-maximum (fwhm) of around 22 cm^{-1} in 1LG, and becomes much stronger, indicating more defects, in the 2−4LG after the hydrogen plasma treatment. The peak at 1620 cm^{-1} is called D′ band, which takes place *via* an intravalley double-resonance process only in the presence of defects.[13] D′ peak is rather weak in 1LG but strong in 2−4LG so that it merges into G band as a shoulder. The weak peak near 2920 cm^{-1} is assigned to D + G band,[17] which is a combination of D mode and G mode. The observation of D, D′ and D + G bands indicate that defects were introduced into the graphene lattice by the hydrogen plasma treatment. This should be caused by hydrogenation of graphene, which results in the formation of C−H sp^3 bonds as well as the breaking of the translational symmetry of C═C sp^2 bonds.[11]

Our capacitively coupled radio frequency hydrogen plasma is operated at moderate pressure (1 Torr) and low power density (0.03 W/cm^2). At this highly collisional condition, the ion bombardment energy is in the range of 5−15 eV.[18,19] The ionization rate is below 0.1% and the concentration of proton (H^+), H_3^+ and the hydrogen radicals (H atoms) are close to 0.0001%, 0.1%, and 1%, respectively.[18,19] During the short hydrogenation process (1 min), we may attribute the hydrogena-

tion of graphene to the contribution of the dominant species, H_3^+ and hydrogen radicals, and ignore the situation that the energetic proton (H^+) might overcome the energy barrier (3.7 eV) to penetrate the center of the hexagonal carbon.[20] Therefore, it is acceptable to assume that the hydrogenation happens only on the top graphene layer of the graphene sheets and the intensity of the D band is proportional to the hydrogen coverage on the top graphene layer. As shown in Figure 1b, it is obvious that, under the 10 W hydrogen plasma treatment, the D band intensity and hence the hydrogen coverage on 2−4LG are much higher than that on 1LG. This conclusion seems to differ from that reported in recent literature, in which hydrogenation is more feasible on 1LG than that on 2LG.[11,21] This difference might be the result of different hydrogenation conditions. The graphene samples in ref 11 and ref 21 were hydrogenated by hydrogen atoms generated by remote hydrogen plasma and electron-induced dissociation of hydrogen silsesquioxane (HSQ), respectively. Our graphene samples were directly exposed to the hydrogen plasma and immersed in the ocean of hydrogen ions (mostly the H_3^+) and hydrogen radicals, where the hydrogen radicals become energetic through the collision with energetic ions (H^+ and H_3^+) in the sheath of hydrogen plasma operated at the moderate pressures.[18] On the contrary, the hydrogen atoms produced in the above two hydrogenation conditions are not so energetic, and the hydrogenation of 1LG was believed to be facilitated by the high activity of a convex surface in the rippled graphene.[11,21]

The DFT study shows that binding a H atom on top of a C atom will shift the C atom around 0.3 Å along the *Z* direction, resulting in an energy barrier of 0.2 eV for chemisorption of atomic H on graphite/multilayer graphene.[22] It is hard for the inactive atomic H produced by the hydrogenation approaches in ref 11 and 21 to overcome this energy barrier. Thanks to the intrinsic rippled atomic structure of 1LG,[23] a small amount of C atoms on the convex surface can chemisorb the H atoms with very small or no barriers, as the lattice of these C atoms is already deformed in the direction that favors sp3 bonding, which lowers the total energy.[11] However, further hydrogenation of C atoms in other parts of 1LG still need to overcome an energy barrier. Therefore, unlike the graphite surface, 1LG has an nonuniform distribution of hydrogenation barriers. The hydrogenation process of 1LG by inactive H atoms might be attributed to the preferential sticking mechanism, which was demonstrated in the hydrogenation process on the graphite surface and recent DFT investigation in hydrogenation of graphene.[24−26] After the fist H atom is chemisorbed by a C atom on the convex surface with a very small barrier, the adsorption barrier for subsequent H in the vicinity of the already adsorbed H atoms further reduces or even vanishes due to H−H interaction,[24−26] which will cause the H atoms to stick

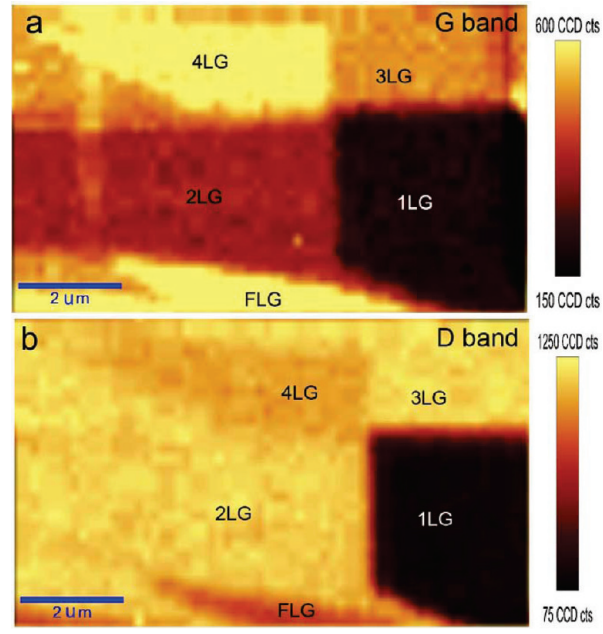

Figure 2. (a) G band intensity Raman image of the pristine graphene sheet; (b) D band intensity Raman image of the graphene sheet hydrogenated by 10 W, 1 Torr hydrogen plasma for 1 min.

on C atoms step by step to form the hydrogenated clusters surrounded by non-hydrogenated C atoms, namely, non-uniform hydrogenation of 1LG reported recently.[11] The hydrogenation rate of this approach is relatively slow, which is consistent with the observation in ref 11 that hydrogenation duration is typically 2 h for reaching the saturation state with the intensity ratio of D and G band at around 1. For 2LG with less rippled atomic structure,[23] the preferential sticking hydrogenation mechanism can not populate substantial H atoms due to the lacking of "the first H atoms" chemisorbed by C atoms on convex surface. Different from the preferential sticking hydrogenation of graphene layers by atomic hydrogen, which shows clear dependence on the corresponding chemical reactivity, hydrogenation of graphene layers by the energetic species in hydrogen plasma should depend on corresponding energy barriers.[22] Under the same hydrogenation condition, the different hydrogen coverage on 1LG and 2LG indicates the corresponding hydrogenation barriers differ from each other.

After vacuum annealing of the hydrogenated graphene at 500 °C for 30−45 min, almost all of the Raman bands related to the defects (D, D′, D + G) induced by hydrogenation can be eliminated, as shown in Figure 1c. It clearly shows that the defects induced by hydrogenation of graphene are reversible and can be thermally healed to restore the original graphene lattice. It was noticed that the dehydrogenation of graphene layers starts at the temperatures as low as 75−100 °C and dehydrogenation can be completed at 350 °C with long annealing duration. The detailed dehydrogenation study will be shown later. Compared with

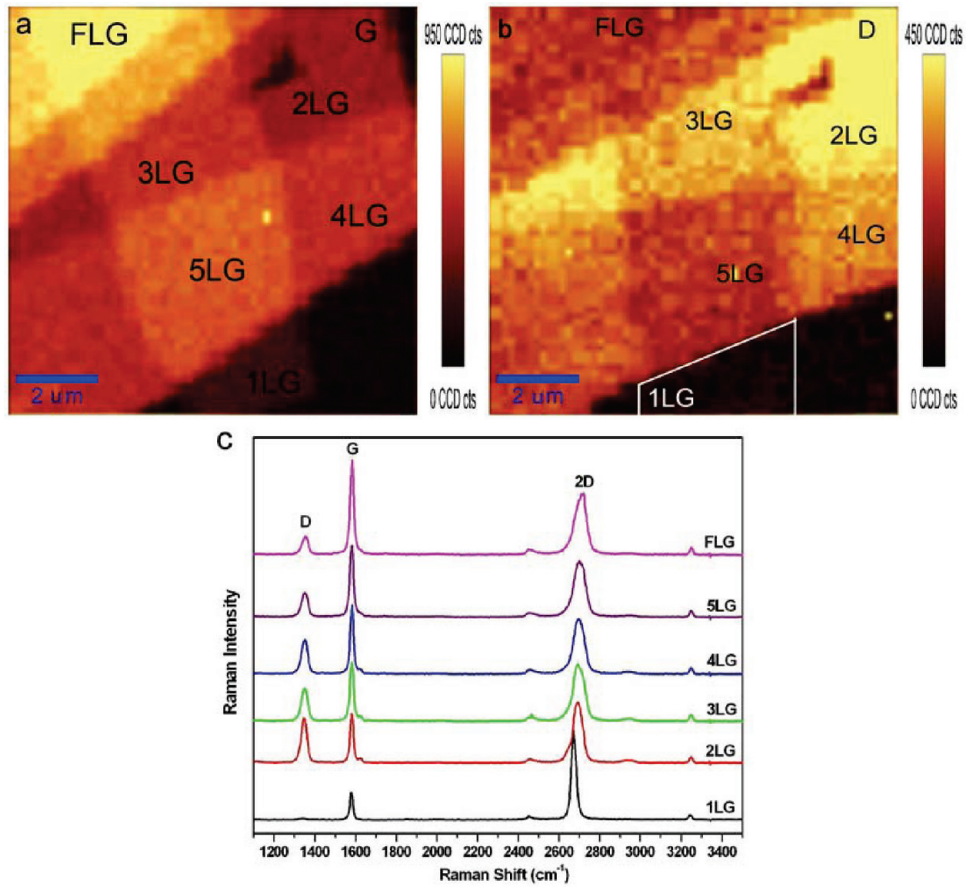

Figure 3. (a) G band intensity Raman image of a pristine graphene sheet; (b) D band intensity Raman image of the graphene sheet hydrogenated by hydrogen diffusing plasma (30 W, 1 Torr, 1 min); (c) Raman spectra of the hydrogenated graphene layers as a function of layer numbers.

the initial Raman spectra shown in Figure 1a, after high temperature vacuum annealing, the intensity of 2D band in Figure 1c decreased and the fwhm of 2D band became broader; moreover, the G and 2D band peaks of one-layer graphene show a strong blue shift, which should be attributed to the hole doping by adsorbing molecular oxygen after exposing the annealed graphene samples to atmosphere.[27]

In Figure 2a, Raman images generated by extracting the G band integrated intensity of the aforementioned graphene sample show clear contrast of the graphene sheets with various layer numbers at five different locations of the SiO_2/Si substrate. With Raman spectra and contrast spectra characterization, these five regions are identified as one-, two-, three-, four- and few (<10)-layer graphene, which are marked as 1LG, 2LG, 3LG, 4LG, and FLG in Figure 2a. Figure 2b shows the Raman image generated from the integrated intensity of D band of the same area after hydrogenation. It is interesting to find that the hydrogen coverage on 2LG and 3LG is higher than that of 1LG and 4LG. Moreover, for the graphene of four and more than four layers, the D band absolute integrated intensity decreases with the increase of graphene thickness, but still much higher than that of 1LG. This complex D band intensity evolution of the hydrogened graphene layers with the number of layers is totally different from the monotonous intensity evolution of D band induced by other defects, such as oxidization by O_2 and particle bombardment.[27,28] The phenomenon that hydrogenation of 2LG and 3LG is more feasible than that of 1LG and 4LG on SiO_2/Si substrate indicates there is a transition number of the graphene layers with the lowest hydrogenation barrier.

The hydrogenation behavior of graphene layers was also studied with H_2 diffusion plasma (30 W, 1 Torr, 1 min), using a Cu plate with small holes (hole size, ~0.5 mm) placed 2 mm above the graphene samples. The grounded Cu plate with small holes can block most of the hydrogen ions and radicals from hydrogen plasma and then can reduce the density of hydrogen ions and radicals in the covered region, resulting in a much slower hydrogenation rate of graphene layers. Figure 3a,b presents the G and D bands intensity image of a graphene sheet that contains one to five layers of graphene with the number of layers marked in the corresponding regions. The Raman spectra taken from 1LG, 2LG, 3LG, 4LG, 5LG, and FLG after hydrogenation were shown in Figure 3c. It is clearly shown that at this relatively mild hydrogenation condition, the D

band intensity of hydrogenated 2LG is the highest and the D band intensity decreases with increased graphene layers. There is no obvious D band in the Raman spectra of 1LG, however the D band in the Raman spectra of multilayer graphene is obvious. The evolution of D band intensity with the number of graphene layers here reconfirms the phenomenon that the hydrogen coverage is different on the graphene with different layers. Under the same plasma environment, different hydrogen coverage should be caused by different hydrogenation barriers. A recent DFT calculation demonstrates a hydrogenation barrier of 0.53 eV for 1LG,[29] which is larger than the value of 0.2 eV for the graphite surface.[22] The layer number depended hydrogenation barriers of graphene layers need further intensive DFT investigation.

For our capacitively coupled radio frequency hydrogen plasma configuration operated at moderate pressure (1 Torr) and low power density (0.03−0.1 W/cm^2), it is safe to expose the graphene layers directly to the plasma. In fact, the threshold energies for sputtering off carbon atoms in graphite by hydrogen ions was calculated to be about 36 eV,[30] which is above the upper limit value for the ion bombardment energy distribution in our hydrogen plasma.[18,19] By monitoring with the D band-integrated intensity of the graphene layers and accordingly modulating the plasma powers and process durations, the hydrogen coverage on the graphene layers can be engineered, as shown in Figure 4. In our plasma configuration, the 1LG can resist the ion bombardment in 30−40 W hydrogen plasma with reversible hydrogenation. According to their lower hydrogenation barriers, multilayer graphenes, particularly the 2LG and 3LG, can reach their saturated hydrogen coverage much faster than the 1LG. It was observed that the hydrogen coverage of 2LG and 3LG with reversible hydrogenation saturate with the plasma power of 15 W for 1 min duration in our plasma system, whereas the 1LG needs much higher power or longer duration to reach its saturation state. As shown in Figure 4b,c, further hydrogenation of the graphene layers with saturated hydrogen coverage will etch carbon atoms by forming the unstable CH_2 configuration,[7] causing irreversible defects.

The X-ray photoelectron spectra (XPS) of the graphene sheets hydrogenated by 15 W, 1 Torr hydrogen plasma for 1 min was studied using the scanning photoemission microscopy (SPEM) with a microfocused beam (1 μm). The C 1s core-level spectra of hydrogenated 1LG, 3LG, and 5LG are shown in Figure 5. The C 1s spectra were fitted with three components: the main peak at a binding energy (BE) of 284.4 eV is assigned to sp2 hybridized C atoms in graphene;[31] another peak at higher BE of 285.05 eV is assigned to sp3 hybridized C atoms due to the formation of C−H and C−C bonds by hydrogenation;[31] the other component with lower BE at 283.5 is very weak, which may originate from the

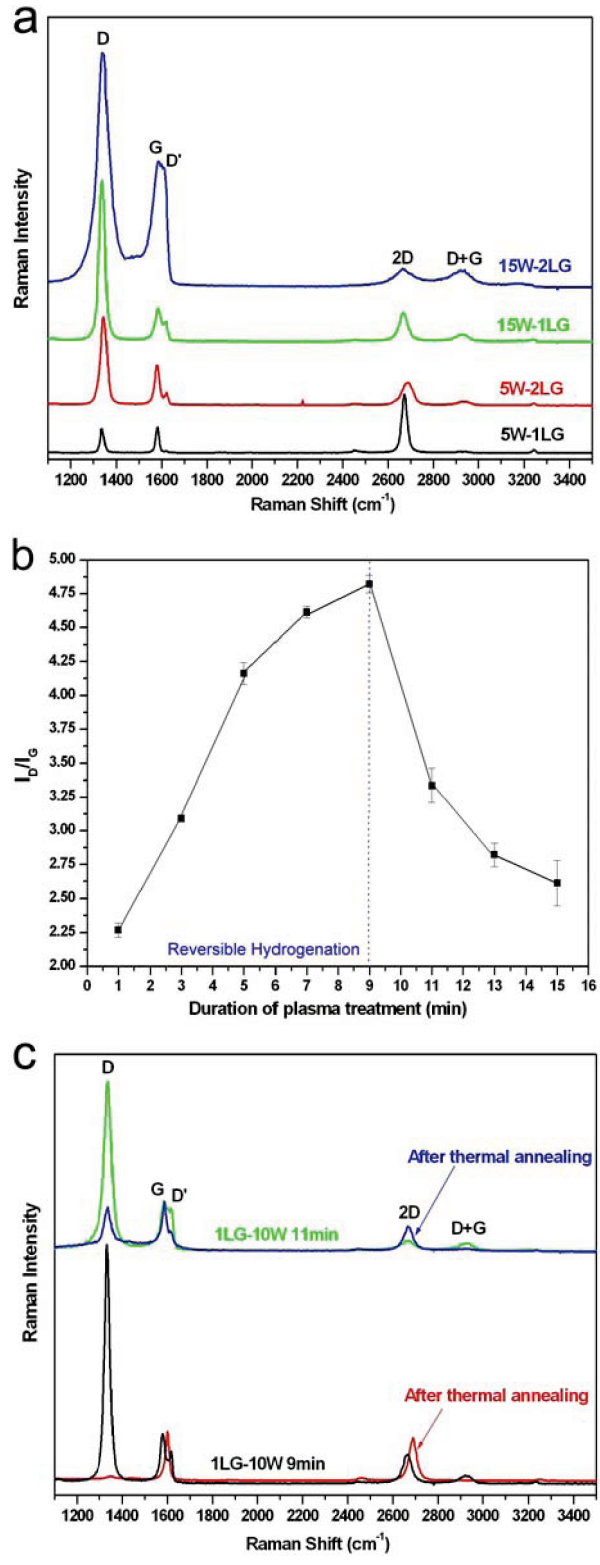

Figure 4. (a) Raman spectra of 1LG and 2LG hydrogenated by 5 and 15 W, 1 Torr hydrogen plasma for 1 min; (b) the evolution of D and G band intensity ratio (I_D/I_G) of 1LG with different process durations under 10 W, 1 Torr hydrogen plasma; (c) Raman spectra of hydrogenated and dehydrogenated state of 1LG treated with 10 W, 1 Torr hydrogen plasma for 9 and 11 min.

interface states and doping effect.[32,33] For 1LG, the intensity ratio of sp3- and sp2-hybridized carbon components is 0.2, corresponding to the hydrogen coverage

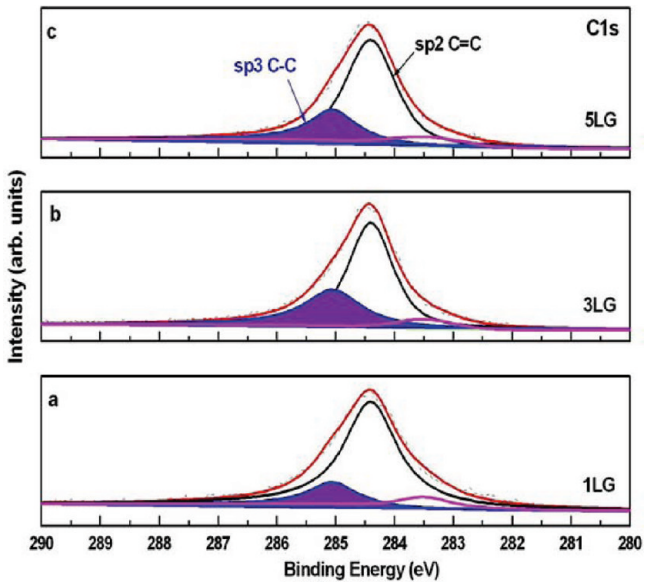

Figure 5. C 1s core-level X-ray photoelectron spectra of 1LG, 3LG, and 5LG hydrogenated by 15 W, 1 Torr hydrogen plasma for 1 min.

of 0.2/1.2 = 16.67%, where 100% hydrogen coverage means every carbon atom in the top layer of graphene layers was hydrogenated.[31] At an excitation energy of E_{hv} = 630 eV, C1s photoelectrons have an E_{kin} = 345 eV and the corresponding attenuation length (λ) is about 8 Å.[34] With the electron escape depth of 4.6 Å ($d = \lambda \cos \theta = 55°$) and the graphene interlayer distance of 3.4 Å, we can roughly estimate that the signal from the top graphene layer contributes 60% and 55% for the sp2 component intensity of 3LG and 5LG, respectively.[34] The intensity ratio of sp3- and sp2-hybridized carbon components of 3LG and 5LG are 0.5 and 0.3, respectively. Therefore, the hydrogen coverages of 3LG and 5LG are 0.5/(0.5 + 1 × 0.6) = 45.5% and 0.3/(0.3 + 1 × 0.55) = 35.3%, respectively.[31] We noted that the hydrogen coverage of 3LG here is close to the saturation coverage on HOPG surface (~50%).[24,35] The hydrogen coverage of 3LG is the largest among the three graphene layers we studied; the hydrogen coverage of 5LG decreased but is still significantly higher than that of 1LG, which is constant with our Raman imaging observation in Figure 2b. The XPS characterization offers a strong support for the above conclusion that the hydrogenation barriers of graphene layers are dependent on the layer number of graphene layers.

The dehydrogenation of graphene layers with different hydrogen coverage, that is, graphene layers hydrogenated with 5 and 15 W, 1 Torr hydrogen plasma for 1 min, was studied with *in situ* Raman spectroscopy. After thermal annealing in vacuum, the Raman D band decreases in intensity relative to the G band, and the fwhm of the G and the 2D band slowly was restored to its pristine state. The I_D/I_G ratio (integrated intensity) starts to exhibit an obvious decrease with the annealing temperature as low as 75 °C, as shown in Figure 6a,c. Such a low dehydrogenation temperature (100 ≈ 200 °C) of the slightly hydrogenated graphene was also recently observed by Ryu *et al.*[21] However, for our hydrogenated graphene samples with low hydrogen coverage, an interesting phenomenon is observed: when the samples are annealed with the increased temperature around 175−200 °C, the I_D/I_G ratio nearly remains unchanged, which means the residual defects cannot be thermally healed with the annealing temperature below 200 °C. With increased annealing temperature, I_D/I_G ratio again starts to decrease rapidly and at last the D band vanishes completely. It seems that there are two stages for the dehydrogenation process (I and II marked in Figure 5a,c) with a boundary at around 175−200 °C, which should correspond to two types of dehydrogenation mechanisms with different dehydrogenation barriers, similar to the dehydrogenation process of graphite surface.[35,36]

To further study of the above-mentioned phenomenon, $\Delta(I_D/I_G)$, the difference in I_D/I_G at two adjacent annealing temperatures, was plotted with the annealing temperature (Figure 6b,d). The fitting curves appear similar to the thermal desorption spectra (TDS) of hydrogen on graphite surface.[35] In fact, with the hypothesis that the D band-integrated intensity of the graphene layers within medium hydrogen coverage is linearly proportional to hydrogen coverage, Figure 5b and Figure 5d should be similar as the thermal desorption spectra with very low heating rate (50 K/1800 s). The thermal desorption spectra of hydrogen on graphite surface was interpreted with first order rate law, in which the dehydrogenation barriers show direct proportion to the desorption peak of annealing temperatures.[35] If the dehydrogenation of graphene also follows the first order rate law, the temperature peak in Figure 6b and Figure 6d can be used to roughly estimate the dehydrogenation barriers. As shown in Figure 6b,d, the desorption peak, that is, the dehydrogenation barrier, of the dehydrogenation process I increases with increased hydrogen coverage, which should be attributed to the H−H interaction at high hydrogen coverage.[35,36] The dehydrogenation barrier of 2LG in dehydrogenation process II is close to that of hydrogenated graphite surface,[35,36] and larger than that of 1LG. This is consistent with recent DFT calculations that for single-side hydrogenation, hydrogenated 2LG has a more stable structure than that of 1LG.[29] It should be noted that, for the highly hydrogenated graphene layers with saturated hydrogen coverage, such as 2LG hydrogenated by 15 W plasma, the hydrogen can also be totally healed by thermal annealing.

CONCLUSION

In conclusion, the hydrogenation of graphene layers by hydrogen plasma is reversible, even at its saturated hydrogen coverage. The hydrogen coverage can be engineered by modulating the parameters such as plasma power and process duration, and the hydroge-

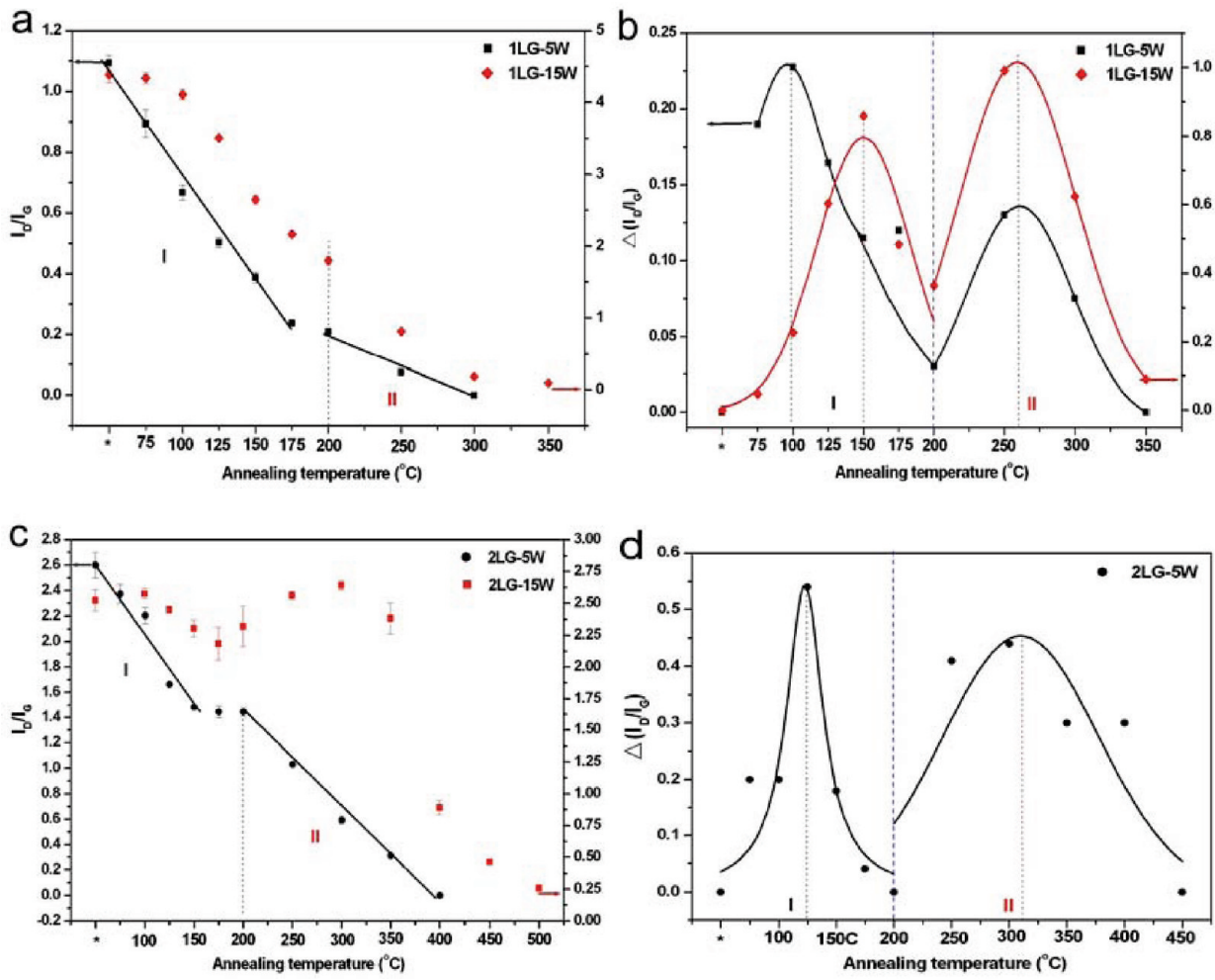

Figure 6. (a) The evolution of the D and G band intensity ratio (I_D/I_G) with annealing temperatures of 1LG hydrogenated by 5 and 15 W, 1 Torr hydrogen plasma for 1 min; (b) the evolution of $\Delta(I_D/I_G)$ with annealing temperatures of 1LG hydrogenated by 5 and 15 W, 1 Torr hydrogen plasma for 1 min; (c) the evolution of the D and G band intensity ratio (I_D/I_G) with annealing temperatures of 2LG hydrogenated by 5 and 15 W, 1 Torr hydrogen plasma for 1 min; (d) the evolution of $\Delta(I_D/I_G)$ with annealing temperatures of 2LG hydrogenated by 5 and 15W, 1 Torr hydrogen plasma for 1 min. The asterisk (*) denotes the as-treated sample by H_2 plasma.

nation rate of graphene layers is controlled by the hydrogenation energy barriers, which show clear dependence on the number of layers. The Raman spectra and micro-XPS spectra investigation demonstrates that the hydrogenation of bilayer and multilayer graphene is much more feasible than that of single layer graphene on SiO_2/Si substrate. Moreover, it was revealed that there are two types of dehydrogenation mechanisms with different dehydrogenation barriers, which show significant dependence on the layer number of graphene sheets and the amount of the hydrogen coverage. Our study provides useful information for exploiting the decorated graphene by grafting exotic atoms and functional groups *via* plasma techniques.

EXPERIMENTAL SECTION

Graphene flakes on Si wafer substrate with a 300 nm SiO_2 cap layer were prepared by mechanical cleavage of highly ordered pyrolytic graphite (HOPG). Optical microscopy was used to locate the graphene flakes. The graphene sheets of one to five layers were confirmed by Raman and contrast spectroscopy/image on a WITEC CRM200 Raman system using a 100× objective lens with a numerical aperture (NA) of 0.95.[12] The excitation source for Raman spectroscopy is a 532 nm laser (2.33 eV) with a laser power below 1 mW to avoid laser-induced heating. Illumination source for the contrast spectroscopy is normal white light. For Raman imaging, the sample was placed on an $X-Y$ piezostage and scanned under the illumination of laser light with a step size of 200 nm. To hydrogenate the graphene flakes, the graphene samples were directly immersed in hydrogen plasma at 1 Torr (133 Pa) with different input powers and process duration. The hydrogen plasma was ignited between two metallic parallel-plate electrodes of 20 cm in diameter and 4 cm separation in a capacitively coupled radio frequency (13.56 MHz) PECVD reactor. X-ray photoelectron spectroscopy of the hydrogenated graphene sample was performed using the 8A1 beamline of the Pohang Accelerator Laboratory in Korea with an incident photon energy of 630 eV and beam size of 1 um. The C 1s core-level spectra were measured with an incident angle of 0° and an emission angle of 55°, where the angle is 0° when the directions are perpendicular to the surface. The dehydrogenation process was studied *in situ* in high temperature and vacuum by Raman spectroscopy performed in a thermal stage (Linkam TS1500) with

the base vacuum pressure of 0.5 Pa. The sample was rapidly heated (50 °C/min) to the desired annealing temperature and then annealed for 30 min. The dehydrogenation in vacuum was repeated with annealing temperature from 75 to 500 °C.

REFERENCES AND NOTES

1. Novoselov, K. S.; Geim, A. K.; Morozov, S. V.; Jiang, D.; Zhang, Y.; Dubonos, S. V.; Grigorieva, I. V.; Firsov, A. A. Electric Field Effect in Atomically Thin Carbon Films. *Science* **2004**, *306*, 666–669.
2. Lin, Y. M.; Jenkins, K. A.; Garcia, A. V.; Small, J. P.; Farmer, D. B.; Avouris, P. Operation of Graphene Transistors at Gigahertz Frequencies. *Nano Lett.* **2009**, *9*, 422–426.
3. Schedin, F.; Geim, A. K.; Morozov, S. V.; Hill, E. W.; Blake, P.; Katsnelson, M. I.; Novoselov, K. S. Detection of Individual Gas Molecules Adsorbed on Graphene. *Nat. Mater.* **2007**, *6*, 652–655.
4. Mohanty, N.; Berry, V. Graphene-Based Single-Bacterium Resolution Biodevice and DNA Transistor: Interfacing Graphene Derivatives with Nanoscale and Microscale Biocomponents. *Nano Lett.* **2008**, *8*, 4469–4476.
5. Bahr, J. L.; Tour, J. M. Covalent Chemistry of Single-Wall Carbon Nanotubes. *J. Mater. Chem.* **2002**, *12*, 1952–1958.
6. Khare, B. N.; Wilhite, P.; Quinn, R. C.; Chen, B.; Schingler, R. H.; Tran, B.; Imanaka, H.; So, C. R.; Bauschlicher, Jr. C. W.; Meyyappan, M. Functionalization of Carbon Nanotubes by Ammonia Glow-Discharge: Experiments and Modeling. *J. Phys. Chem. B* **2004**, *108*, 8166–8172.
7. Zhang, G.; Qi, P.; Wang, X.; Lu, Y.; Mann, D.; Li, X.; Dai, H. Hydrogenation and Hydrocarbonation and Etching of Single-Walled Carbon Nanotubes. *J. Am. Chem. Soc.* **2006**, *128*, 6026–6027.
8. Zheng, G.; Li, Q.; Jiang, K.; Zhang, X.; Chen, J.; Ren, Z.; Fan, S. Transition of Single-Walled Carbon Nanotubes from Metallic to Semiconducting in Field-Effect Transistors by Hydrogen Plasma Treatment. *Nano Lett.* **2007**, *7*, 1622–1625.
9. Boukhvalov, D. W.; Katsnelson, M. I. Tuning the Gap in Bilayer Graphene Using Chemical Functionalization: Density Functional Calculations. *Phys. Rev. B* **2008**, *78*, 085413/1−085413/5.
10. Sofo, J. O.; Chaudhari, A. S.; Barber, G. D. Graphane: A Two-Dimensional Hydrocarbon. *Phys. Rev. B* **2007**, *75*, 153401/1−153401/4.
11. Elias, D. C.; Nair, R. R.; Mohiuddin, T. M. G.; Morozov, S. V.; Blake, P.; Halsall, M. P.; Ferrari, A. C.; Boukhvalov, D. W.; Katsnelson, M. I.; Geim, A. K.; Novoselov, K. S. Control of Graphene's Properties by Reversible Hydrogenation: Evidence for Graphane. *Science* **2009**, *323*, 610–613.
12. Ni, Z. H.; Wang, H. M.; Kasim, J.; Fan, H. M.; Yu, T.; Wu, Y. H.; Feng, Y. P.; Shen, Z. X. Graphene Thickness Determination Using Reflection and Contrast Spectroscopy. *Nano Lett.* **2007**, *7*, 2758–2763.
13. Ferrari, A. C. Raman Spectroscopy of Graphene and Graphite: Disorder, Electron-Phonon Coupling, Doping and Nonadiabatic Effects. *Solid State Commun.* **2007**, *143*, 47–57.
14. Ferrari, A. C.; Meyer, J. C.; Scardaci, V.; Casiraghi, C.; Lazzeri, M.; Mauri, F.; Piscanec, S.; Jiang, D.; Novoselov, K. S.; Roth, S.; Geim, A. K. Raman Spectrum of Graphene and Graphene Layers. *Phys. Rev. Lett.* **2006**, *97*, 187401/1−187401/4.
15. Graf, D.; Molitor, F.; Ensslin, K.; Stampfer, C.; Jungen, A.; Hierold, C.; Wirtz, L. Spatially Resolved Raman Spectroscopy of Single- and Few-Layer Graphene. *Nano Lett.* **2007**, *7*, 238–242.
16. Wang, Y. Y.; Ni, Z. H.; Shen, Z. X.; Wang, H. M.; Wu, Y. H. Interference Enhancement of Raman Signal of Graphene. *Appl. Phys. Lett.* **2008**, *92*, 043121/1−043121/3.
17. Pimenta, M. A.; Dresselhaus, G.; Dresselhaus, M. S.; Cancado, L. G.; Jorioa, A.; Saitoe, R. Studying Disorder in Graphite-Based Systems by Raman Spectroscopy. *Phys. Chem. Chem. Phys.* **2007**, *9*, 1276–1291.
18. Lieberman, M. A.; Lichtenberg, A. J. Principles of Plasma Discharges and Materials Processing; Wiley: New York, 1994; pp 327−353.
19. Nunomura, S.; Kondo, M. Characterization of High-Pressure Capacitively Coupled Hydrogen Plasmas. *J. Appl. Phys.* **2007**, *102*, 093306/1−093306/7.
20. Zhou, Y. G.; Zu, X.; Gao, T. F.; Nie, J. L.; Xiao, H. Y. Adsorption of Hydrogen on Boron-Doped Graphene: A First-Principles Prediction. *J. Appl. Phys.* **2009**, *105*, 014309/1−014309/4.
21. Ryu, S.; Han, M. Y.; Maultzsch, J.; Heinz, T. F.; Kim, P.; Steigerwald, M. L.; Brus, L. E. Reversible Basal Plane Hydrogenation of Graphene. *Nano Lett.* **2008**, *8*, 4597–4602.
22. Sha, X.; Jackson, B. First-Principles Study of the Structural and Energetic Properties of H Atoms on a Graphite (0001) Surface. *Surf. Sci.* **2002**, *496*, 318–330.
23. Meyer, J. C.; Geim, A. K.; Katsnelson, M. I.; Novoselov, K. S.; Booth, T. J.; Roth, S. The Structure of Suspended Graphene Sheets. *Nature* **2007**, *446*, 60–63.
24. Hornek, L.; Rauls, E.; Xu, W.; Sljivancanin, Z.; Otero, R.; Stensgaard, I.; Lægsgaard, E.; Hammer, B.; Besenbacher, F. Clustering of Chemisorbed H(D) Atoms on the Graphite (0001) Surface due to Preferential Sticking. *Phys. Rev. Lett.* **2006**, *97*, 186102/1−186102/4.
25. Lin, Y.; Ding, F.; Yakobson, B. I. Hydrogen Storage by Spillover on Graphene as a Phase Nucleation Process. *Phys. Rev. B* **2008**, *78*, 041402/1−041402/4.
26. Casolo, S.; Lovvik, O. M.; Martinazzo, R.; Tantardini, G. F. Understanding Adsorption of Hydrogen Atoms on Graphene. *J. Chem. Phys* **2009**, *130*, 054704/1−054704/10.
27. Liu, L.; Ryu, S.; Tomasik, M. R.; Stolyarova, E.; Jung, N.; Hybertsen, M. S.; Steigerwald, M. L.; Brus, L. E.; Flynn, G. W. Graphene Oxidation: Thickness-Dependent Etching and Strong Chemical Doping. *Nano Lett.* **2008**, *8*, 1965–1970.
28. Ni, Z. H.; Wang, H. M.; Ma, Y.; Kasim, J.; Wu, Y. H.; Shen, Z. X. Tunable Stress and Controlled Thickness Modification in Graphene by Annealing. *ACS Nano* **2008**, *2*, 1033–1039.
29. Boukhvalov, D. W.; Katsnelson, M. I.; Lichtenstein, A. I. Hydrogen on Graphene: Electronic Structure, Total Energy, Structural Distortions and Magnetism from First-Principles Calculations. *Phys. Rev. B* **2008**, *77*, 035427/1−035427/7.
30. Bohdansky, J.; Roth, J.; Bay, H. L. An Analytical Formula and Important Parameters for Low-Energy Ion Sputtering. *J. Appl. Phys.* **1980**, *51*, 2861–2865.
31. Nikitin, A.; Naslund, L.; Zhang, Z.; Nilsson, A. C-H Bond Formation at The Graphite Surface Studied with Core Level Spectroscopy. *Surf. Sci.* **2008**, *602*, 2575–2580.
32. Kim, K.; Choi, J.; Lee, H.; Lee, H.; Kang, T.; Han, Y.; Lee, B.; Kim, S.; Kim, B. Effects of 1 MeV Electron Beam Irradiation on Multilayer Graphene Grown on 6H-SiC(0001). *J. Phys. Chem. C* **2008**, *112*, 13062–13064.
33. Bekyarova, E.; Itkis, M. E.; Ramesh, P.; Berger, C.; Sprinkle, M.; de Heer, W. A.; Haddon, R. C. Chemical Modification of Epitaxial Graphene: Spontaneous Grafting of Aryl Groups. *J. Am. Chem. Soc.* **2009**, *131*, 1336–1337.
34. Hufner, S. Photoelectron Spectroscopy: Principles and Applications; Springer-Verlag: Berlin, Heidelberg, 1996; pp 8−10.
35. Zecho, T.; Guttler, A.; Sha, X.; Jackson, B.; Kuppers, J. Adsorption of Hydrogen and Deuterium Atoms on the (0001) Graphite Surface. *J. Chem. Phys.* **2002**, *117*, 8486–8492.
36. Hornek, L.; Sljivancanin, Z.; Xu, W.; Otero, R.; Rauls, E.; Stensgaard, I.; Lægsgaard, E.; Hammer, B.; Besenbacher, F. Metastable Structures and Recombination Pathways for Atomic Hydrogen on the Graphite (0001) Surface. *Phys. Rev. Lett.* **2006**, *96*, 156104/1−156104/4.